

Using Polarity for Engineering Oxide Nanostructures: Structural Phase Diagram in Free and Supported MgO(111) Ultrathin Films

Jacek Goniakowski* and Claudine Noguera

Groupe de Physique des Solides, UMR 7588 CNRS and Universités Paris 6 - Paris 7, Campus de Bouicaut, 140 rue de Lourmel, 75015 Paris, France

Livia Giordano

Dipartimento di Scienza dei Materiali, Università di Milano-Bicocca, Via R. Cozzi, 53, 20125 Milano, Italy
(Received 21 July 2004; published 17 November 2004)

Using an *ab initio* total energy approach, we study the stability of free and Ag(111)-supported MgO(111) ultrathin films. We unravel a novel microscopic mechanism of stabilization of polar oxide orientations, based on a strong modification of the MgO structural phase diagram with respect to the bulk material. We predict that, at low thickness, films which are either unsupported or deposited on Ag(111) display a graphitelike B_k structure rather than the expected rocksalt one. Our results provide a consistent interpretation of recent experimental findings, exemplify the efficiency of this novel stabilization mechanism, and suggest new methods to engineer oxide nanostructures.

DOI: 10.1103/PhysRevLett.93.215702

PACS numbers: 64.70.Nd, 68.55.Jk, 81.30.Dz

The latest advances in the fabrication of artificial materials and in nanoengineering techniques question our fundamental understanding of low dimensionality effects in materials which are at present mainly known for their bulk or surface properties. This is especially true for oxide nanostructures, which, in the past, have attracted less consideration than their semiconductor or metal counterparts.

Indeed, unraveling the competition between different atomic structures in bulk binary *sp*-bonded compounds has required long-standing efforts in the last decades. It is well established that crystallization usually occurs in one of the following forms: rocksalt (B1), cesium chloride (B2), zinc blende (B3), and wurzite (B4). However, other forms exist, such as an hexagonal graphitelike (B_k) form, which appears as a transition phase in pressure-induced $B4 \rightarrow B1$ and $B3 \rightarrow B1$ transformations in MgO [1].

Compared to bulk materials, ultrathin films not only involve many undercoordinated atoms. Their interaction with the substrate also provides constraints on their orientation and often yields an elastic stress, equivalent to an applied pressure. These three factors may noticeably modify their structural properties with respect to the bulk. Thus, adapting the nature of the substrate, the orientation of its surface, and the thickness of the deposited films can be seen as the most promising directions towards synthesizing artificial materials, with no bulk equivalent and with new properties.

In the field of oxides, several results of successful growth of ultrathin films of dense orientations have been reported [2]. However, these dense orientations, as, for example, MgO(100), present a moderate interest, since, as soon as the film thickness exceeds two monolayers (MLs), atoms recover an environment similar to that at a semi-infinite surface.

Ultrathin films along *open* and, in particular, *polar* orientations should display stronger peculiarities, but their studies remain scarce [3–7]. We recall that highly ionic semi-infinite polar surfaces cannot be stabilized unreconstructed and defect-free [8]. In this respect, the recent growth of MgO(111) films on Ag(111) [7] proves that obtaining *planar* films with an orientation other than the MgO(100) cleavage one is actually possible. This major experimental breakthrough questions our present understanding of polarity, beyond what is already known for semi-infinite surfaces.

We address here two issues: the role of thickness effects and the possibility of avoiding polarity through a structural transformation in the film. The present study provides the first evidence of an entirely novel mechanism of stabilization of polar ionic nanostructures. In the particular case of the weakly adhesive MgO/Ag interface, we believe it gives an alternative and better founded interpretation of the experiments reported in Ref. [7].

We use the density-functional theory at the gradient-corrected level [9], as implemented in the Vienna *ab initio* simulation package (VASP) [10] with ultrasoft pseudopotentials [11]. A slab geometry is adopted and all atomic degrees of freedom, including film lattice parameters, are relaxed. The energetics of MgO B1, B3, B4, and B_k bulk phases is shown in Fig. 1. We note that on the negative pressure side, B_k is only 0.06 eV/formula unit above B1. All phases are insulating and their charges [12] are close to those of B1.

In order to discriminate between substrate-induced effects and properties inherent to the thin film, we first consider unsupported MgO films with two-dimensional (2D) (1×1) cells corresponding to orientations (111) for B1, B2, and B3, and (0001) for B4 and B_k [for a short notation, referred to as MgO(111)]. The films are neutral

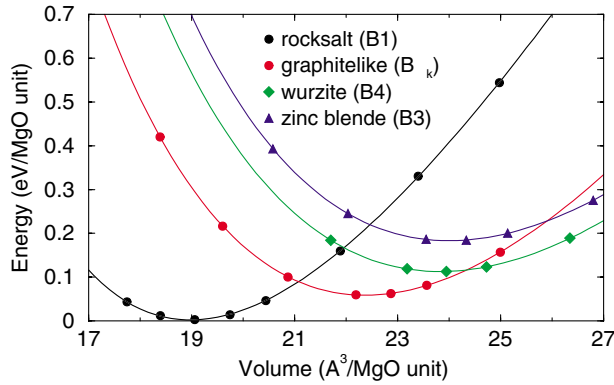


FIG. 1 (color online). Energy of crystalline phases of bulk MgO (eV/MgO formula unit), as a function of volume (\AA^3 /formula unit). The energy zero is taken at the B1 ground state. The cesium-chloride (B2) curve (with its minimum at $V = 18.73 \text{ \AA}^3$ and $E = 1.53 \text{ eV}$) is located beyond the limits of the figure.

and stoichiometric and their thickness N is defined as the number of MgO formula units in the (1×1) 2D cell (number of MgO layers). We stress that for all systems but $B_k(0001)$ (whose anions and cations are coplanar), truncated bulk pieces have a nonvanishing anion to cation intralayer distance (hereafter referred to as rumpling), and thus possess a dipole moment proportional to their thickness—a signature of polar instability.

We also consider (2×2) reconstructed films, assuming a B1 octopolar model [13] or a B3 vacancy model [14], which are the most widely accepted ways to heal polarity at semi-infinite B1 and B3(111) surfaces, respectively. Finally, in order to bridge the gap between perfect hexagonal and fcc stacking, B1 and B3 films with one or several stacking faults are modeled.

Figure 2 shows the film energy per surface area E_f (with respect to MgO B1 bulk) as a function of thickness for $N \leq 4$. E_f is defined as $(E_{\text{film}} - \mathcal{N}E_{\text{bulk}}^{\text{B1}})/A$ (with \mathcal{N} the number of MgO formula units in the film, and A the 2D cell area). With this definition, small E_f values correspond to enhanced stability. Upon geometry optimization, we find that (1×1) B1(111) and B2(111) spontaneously relax towards B3(111), and B4(0001) evolves towards $B_k(0001)$. In this thickness range, the competition thus takes place between hexagonal (B_4 - B_k) and fcc (B1-B3) stacking, with possible stacking faults. At $N = 1$, all relaxed structures are identical.

For $N \leq 4$, the most stable structure is $B_k(0001)$, with almost planar MgO layers. It is insulating and nonpolar, with gap and charges close to their bulk values. Its in-plane lattice parameter a is large, consistently with the stability of the MgO B_k bulk phase at negative pressures; a increases monotonically from 3.26 \AA at $N = 1$ to 3.49 \AA at $N \rightarrow \infty$. The increase of E_f with N is slow (dashed-arrow line in Fig. 2) due to the small energy difference between bulk B_k and B1.

Conversely, E_f rapidly increases with N in fcc(111) films. Although the layer rumpling is equal only to $\approx 9\%$ of the bulk value, fcc films are undoubtedly polar with a dipole moment of the order of $0.05 e\text{\AA}$ per MgO layer. The large value of E_f is due to this residual dipole, to the elastic deformation which reduces the rumpling, and to the difference of bulk cohesion energies between B3 and B1. As expected, B_k films with stacking faults have energies intermediate between purely hexagonal and purely fcc films.

Finally, (2×2) reconstructions efficiently suppress the polarity of fcc films. The octopolar termination turns out to be the most favorable reconstruction. However, while it eventually becomes the ground state at large thicknesses, it is not the lowest energy structure for small N . From the slope of E_f , we predict the transition from hexagonal to (2×2) B1 at $N_c = 30 \pm 4$.

In Fig. 2, we have added results for B1(100) thin films, since, at least in the asymptotic N limit, they are expected to be the lowest energy structures. We note that their energy is not the lowest for $N \leq 2$ and that an energy barrier exists between $B_k(0001)$ and B1(100) structures for all values of N . This result gives support to a possible stabilization of $B_k(0001)$ films of finite thickness, in a stable ($N < 3$) or metastable ($N \geq 3$) state.

To summarize this first part devoted to unsupported films, we have shown that the choice of the MgO(111)

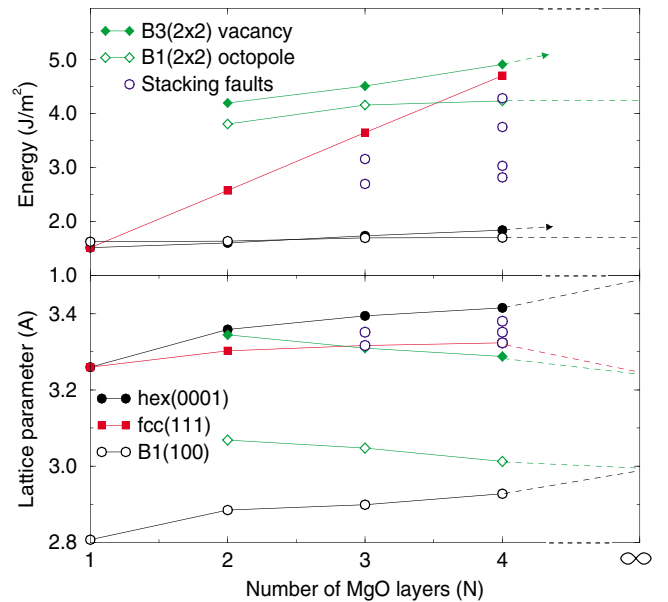


FIG. 2 (color online). MgO film energy per surface area E_f (J/m^2) (with respect to MgO B1 bulk) (top panel) and the in-plane lattice parameter (bottom panel) for various crystallographic structures as a function of the number of MgO layers. Asymptotic values for semi-infinite systems are shown. Dashed lines terminated by arrows indicate the constant energy increase of B3 and B_k films with respect to B1 when thickness increases.

orientation induces a substantial modification of the bulk phase diagram, privileging hexagonal(0001) stacking over polar fcc(111) ones. To our knowledge, this is the first time that such a mechanism is predicted. Being perfectly general, this polarity-induced modification of crystallographic structure can be conceived as a potential tool for engineering ionic nanostructures.

However, in order to confirm our prediction that planar ultrathin MgO(111) films may actually be obtained (meta)stable, as sustained by a recent report of growth on Ag(111) [7], it is necessary to enlarge the above analysis, by taking into account the interfacial interaction with a substrate. This is especially important since a stabilization mechanism of polar oxide surfaces by metal deposition has already been invoked [15].

For this purpose, we have modeled both fcc(111) and hexagonally (0001) stacked MgO thin films on an Ag(111) surface. For both stackings, we have considered two interface structures. First, we have constrained the MgO films to adopt the (1×1) Ag(111) surface unit cell, which is reasonable in view of the small (3%) lattice mismatch which exists between MgO B1 bulk and Ag. Second, we have considered a $(2\sqrt{3} \times 2\sqrt{3})R30^\circ$ 2D unit cell, which is the smallest coincidence cell, which allows a nearly perfect accommodation (2% tension at $N = 1$ and 1% compression at $N = 2$ and 3) of the lattice mismatch between Ag(111) and unsupported $B_k(0001)$ films (Fig. 3). We thus will be able to settle which interface is the most stable: the polar Ag/fcc-MgO(111) with its high-energy oxide film strongly stabilized by interfacial charge redistributions, or the nonpolar Ag/hex-MgO(0001) interface with its low-energy oxide film weakly bound to the substrate.

Table I gives the energy E_f per surface area, referred to the Ag(111) substrate and MgO B1 bulk, of Ag(111)-supported MgO films ($N \leq 3$). It is defined as $(E_{\text{film}/\text{Ag}(111)} - \mathcal{N}E_{\text{bulk}}^{\text{B1}} - E_{\text{Ag}(111)})/A$ (with $E_{\text{Ag}(111)}$ the total energy of the Ag substrate). Systematically, interfaces with a $(2\sqrt{3} \times 2\sqrt{3})R30^\circ$ unit cell have energies by far lower than the (1×1) ones, proving the inadequacy of the (1×1) model. Substrate-induced charge redistributions, similar to those observed at metal/oxide polar interfaces [15] (the reversed system), are thus obviously unable to efficiently stabilize these films. The relative stability of fcc(111) and hexagonal(0001) films in the large unit cell and their energy difference are very similar to those found in unsupported films. This confirms the

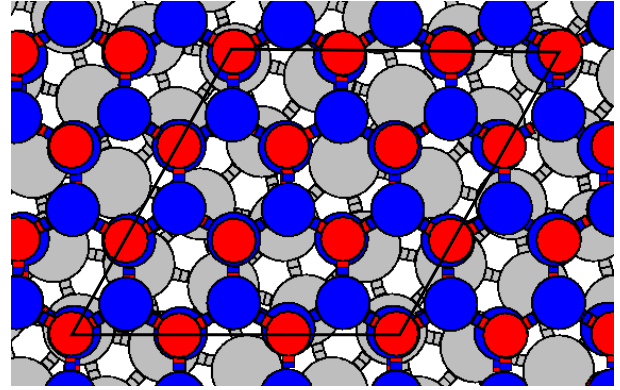


FIG. 3 (color online). Top view of the $(2\sqrt{3} \times 2\sqrt{3})R30^\circ$ graphitelike MgO/Ag(111) interface. Oxygen, magnesium, and silver atoms are drawn in blue (black), red (dark gray), and gray, respectively.

presence of weak adhesion forces and weak elastic stresses at this interface.

In order to complement the picture and to definitely assess the instability of (1×1) interfaces, we have modeled nonstoichiometric B1 films, with a pseudomorphic (1×1) structure at the Ag interface and an octopolar (2×2) reconstruction at the interface with vacuum. The analysis of their stability requires an estimation of their formation grand potential (which we define as $E_f - (\mu_{\text{O}}N_{\text{O}} - \mu_{\text{Mg}}N_{\text{Mg}})/A$, with μ and N being, respectively, the chemical potential and the number of atoms), as a function of the oxygen chemical potential μ_{O} [16]. As shown in Fig. 4, stoichiometric $B_k(0001)$ films in $(2\sqrt{3} \times 2\sqrt{3})R30^\circ$ epitaxy on Ag(111) remain by far the most stable in the largest part of the phase diagram. Only in extremely oxygen-poor conditions may the O-terminated (Mg-rich) reconstructed B1 films become competitive.

We thus conclude that, in most attainable experimental conditions, the B_k structure, predicted to be the ground state of unsupported MgO(111) layers, remains by far the lowest energy structure for MgO on Ag(111). Our model of $(2\sqrt{3} \times 2\sqrt{3})R30^\circ$ epitaxy gives hints that the stable interface is (fully) relaxed. However, the calculated adhesion energy (about 0.2 J/m^2 , independently on the film thickness), together with the $B_k(0001)$ surface energy (0.8 J/m^2) are consistent with a bad wetting of MgO on Ag (wetting angle of the order of 140°), and compatible with a 3D growth mode. The planar geometries studied

TABLE I. Energy per surface area E_f (J/m^2) of Ag(111)-supported MgO ultrathin films, with respect to B1 MgO bulk.

	One ML		Two MLs		Three MLs	
	$(2\sqrt{3} \times 2\sqrt{3})$	(1×1)	$(2\sqrt{3} \times 2\sqrt{3})$	(1×1)	$(2\sqrt{3} \times 2\sqrt{3})$	(1×1)
hex(0001)	1.3	4.2	1.5	6.6	1.7	8.4
fcc(111)	1.3	4.2	2.3	6.8	3.3	7.9

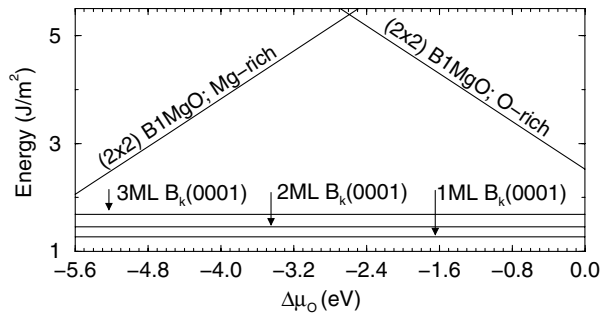


FIG. 4. Formation grand potential per surface area of Ag(111)-supported thin MgO films (J/m^2) as a function of oxygen excess chemical potential $\Delta\mu_{\text{O}}$ (eV).

here and found experimentally thus represent metastable states.

Our results suggest a new interpretation of the experimental findings of Ref. [7], alternative to that proposed by the authors, who assume a (1×1) B1(111) structure. Indeed, at one ML, the nearly perfect planarity of the $B_k(0001)$ solution is consistent with the sharpness of the experimental reflection high-energy electron diffraction patterns. Also the calculated in-plane lattice constant (3.26 \AA), much larger than either that of Ag(111) surface or B1 MgO(111) layers (2.89 and 2.98 \AA , respectively), is in excellent agreement with the experimental data ($3.25 \pm 0.03 \text{ \AA}$). For thicker films, and especially for the case of $N = 5$ detailed in Ref. [7], the authors report an in-plane lattice constant ($3.28 \pm 0.03 \text{ \AA}$) somewhat smaller than what we find (3.43 \AA). Whereas this value is definitely inconsistent with the B1(111) assumption, it can easily be accounted for by the $B_k(0001)$ structure with stacking faults (see the variations of the in-plane lattice parameters induced by stacking faults in Fig. 2). Additionally, while perfect $B_k(0001)$ films are insulating, we find that stacking faults induce a nonzero density of states in the gap, in good agreement with the ultraviolet photoemission spectroscopy and electron-energy-loss spectroscopy experimental spectra. It should be stressed that the kinetic hindering responsible for film growth is consistent with the production of planar films, which, due to the bad wetting, are necessarily in a metastable state.

On a more general level, the present study of MgO ultrathin films clearly shows the relevance of the B_k , graphitelike crystallographic structure for MgO nano-objects. It is in line with results on small $(\text{MgO})_{3n}$ clusters, which have been shown to present nanotube shapes made of superimposed $(\text{MgO})_3$ hexagons [17]. Grains of B_k structure [with (0001) faces perpendicular to the interface] have also been found to reduce the interface mismatch between MgO and $\text{SrTiO}_3(100)$ [18].

In this context, it is worth underlining that, whereas undercoordination effects and elastic stresses have been widely recognized as driving forces for a modification of bulk structural phase diagrams in ultrathin films, in the present study we reveal an entirely new driving force originating in the suppression of polarity. We believe that growth of (metastable) oxide films along polar orientation may represent a novel and powerful way to synthesize artificial materials with unusual crystallographic structure and properties, strongly dependent upon their thickness.

We are grateful to Jacques Jupille, Fabio Finocchi, Gianfranco Pacchioni, and Claude Henry for fruitful discussions. This work was supported by the COST D19 action.

*Electronic address: jacek@gps.jussieu.fr

- [1] M. Wilson and P. A. Madden, *J. Phys. Condens. Matter* **14**, 4629 (2002).
- [2] J. Kramer, C. Tegenkamp, and H. Pfnür, *Phys. Rev. B* **67**, 235401 (2003); L. Savio *et al.*, *Phys. Rev. B* **67**, 75420 (2003); S. Schintke *et al.*, *Phys. Rev. Lett.* **87**, 276801 (2001); Y. D. Kim, J. Stultz, and D. W. Goodman, *Surf. Sci.* **506**, 228 (2002).
- [3] R. Franchy, *Surf. Sci. Rep.* **38**, 195 (2000); R. M. Jaeger *et al.*, *Surf. Sci.* **259**, 235 (1991).
- [4] H. J. Freund, H. Kühlenbeck, and V. Staemmler, *Rep. Prog. Phys.* **59**, 283 (1996); S. K. Shaikhutdinov *et al.*, *Phys. Rev. Lett.* **91**, 076102 (2003).
- [5] W. Weiss and W. Ranke, *Prog. Surf. Sci.* **70**, 1 (2002).
- [6] S. Gota *et al.*, *Phys. Rev. B* **60**, 14387 (1999).
- [7] M. Kiguchi *et al.*, *Phys. Rev. B* **68**, 115402 (2003); R. Arita *et al.*, *Phys. Rev. B* **69**, 235423 (2004).
- [8] C. Noguera, *J. Phys. Condens. Matter* **12**, R367 (2000), and references therein.
- [9] Y. Wang and J. P. Perdew, *Phys. Rev. B* **44**, 13298 (1991).
- [10] G. Kresse and J. Hafner, *Phys. Rev. B* **47**, 558 (1993).
- [11] D. Vanderbilt, *Phys. Rev. B* **41**, 7892 (1990); G. Kresse and J. Hafner, *J. Phys. Condens. Matter* **6**, 8245 (1994).
- [12] R. F. W. Bader, *Chem. Rev.* **91**, 983 (1991).
- [13] D. Wolf, *Phys. Rev. Lett.* **68**, 3315 (1992); F. Finocchi *et al.*, *Phys. Rev. Lett.* **92**, 136101 (2004).
- [14] E. Kaxiras *et al.*, *Phys. Rev. B* **35**, 3625 (1987).
- [15] J. Goniakowski and C. Noguera, *Phys. Rev. B* **60**, 16120 (1999); **66**, 085417 (2002).
- [16] G.-X. Qian, R. M. Martin, and D. J. Chadi, *Phys. Rev. B* **38**, 7649 (1988).
- [17] S. Moukouri and C. Noguera, *Z. Phys. D* **24**, 71 (1992); M.-J. Malliavin and C. Coudray, *J. Chem. Phys.* **106**, 2323 (1997); A. Aguado and J. M. López, *J. Phys. Chem. B* **104**, 8398 (2000).
- [18] D. C. Sayle and G. W. Watson, *J. Phys. Chem. B* **105**, 5506 (2001).